

Figure 1. Structures of fumonisins FB₁, FB₂ and FB₃, hydrolyzed fumonisins (aminopolyols) HFB₁ and HFB₂ and the corresponding *N*-acyl-derivatives.

6] and porcine pulmonary edema [7, 8], respectively. FB₁ is hepatotoxic and nephrotoxic to a variety of species and is a liver and kidney carcinogen in rodents [1, 9–13]. Concerning their impact on humans, fumonisins have been implicated as a possible cause of esophageal cancer in China and South Africa [14, 15] and it has furthermore been hypothesized that fumonisins are a risk factor for neural tube defects (NTD) [16], for which there has been recent epidemiologic evidence [17]. The likely explanation for the ability of fumonisins to have such diverse toxicities is that their mechanism of action is to inhibit ceramide synthase(s), the enzymes catalyzing the acylation of sphinganine and sphingosine to dihydroceramides and ceramides, respectively [18–21]. This disruption of sphingolipid metabolism causes a decrease of complex sphingolipids and an accumulation of highly bioactive sphingoid bases, sphinganine and sphingosine, and their 1-phosphate metabolites [18–22]. The toxicological implications are reviewed elsewhere [18–22].

The hydrolyzed form of FB₁ has also been shown to be an inhibitor of ceramide synthase, but HFB₁ is tenfold less

potent compared to FB₁ and it is cytotoxic, although less toxic than FB₁ in cell culture [23]. There is conflicting evidence concerning the *in vivo* toxicity of hydrolyzed fumonisins. Hepatic and renal lesions found in rats fed hydrolyzed *F. verticillioides* culture materials containing HFB₁ (but no detectable FB₁) were qualitatively similar to those caused by FB₁ [24, 25] whereas purified HFB₁ did not cause liver or kidney apoptosis or disrupt sphingolipid metabolism when fed to female mice [26] or given by gavage to pregnant rats [27]. The reasons underlying these apparently contradictory results have not been established. In studies of the possible mechanisms whereby hydrolyzed fumonisins are toxic, HFB₁ was found to be acylated by ceramide synthase to form the metabolite *N*-palmitoyl-aminopolyol (C₁₆-HFB₁), which was toxic to cells in culture [28]. Since that publication, it has been found that there are multiple isoforms of ceramide synthases (CerS) that differ in fatty acyl-coenzyme A (CoA) selectivity [29–32]. The aims of this study were to further characterize the acylation of HFB₁ and HFB₂ *in vitro*, to study the biological activities of long-chain and very long-chain *N*-acylated hydrolyzed fumonisin metabolites *in vitro*, and to demonstrate that *N*-acylation of HFB₁ occurs *in vivo*.

2 Materials and methods

2.1 Materials

FB₁, FB₂ and HFB₁ were supplied by Dr. M. Trucksess from the US Food and Drug Administration, Washington, DC, USA. HFB₂ was produced from FB₂ according to the method of Hopmans *et al.* [33] and further purified by a C18 cartridge. HFB₁ for the animal experiment was prepared from semipurified FB₁ extracted from *F. verticillioides* culture material (approximately 75% purity; a gift from Filmore Meredith, Toxicology & Mycotoxin Research Unit, Agricultural Research Service-USDA, Athens, GA). Briefly, the FB₁ was dissolved in 2 N KOH and quantitatively transferred (two washes with 2 N KOH) to a Teflon-capped test tube. The tube was shaken, sonicated briefly (<1 min) and heated (70°C) for approximately 20 h. After cooling to ambient temperature, the pH was adjusted to 4.0 using dilute HCl and then brought to volume (110 mL) with deionized water. For cleanup, the HFB₁ solution was loaded onto a preconditioned C18 cartridge. The cartridge was washed with 100 mL water and 100 mL 15% aqueous ACN, after which the HFB₁ was eluted with 100 mL of 70% ACN. Purity (>95%) of the HFB₁ was assessed by comparison of the HFB₁ to an analytical standard by HPLC-MS (SIM) (Stephen Poling, ARS-USDA, Peoria, IL).

Silica gel and C18 SPE columns were purchased from Waters (Milford, MA). *D-erythro*-[3-³H]sphingosine was from NEN Life science Products. All other chemicals were of reagent grade.

2.2 Analytical methods

HPLC-ESI-MS/MS analysis of ceramide synthase acylation products were performed on a Perkin-Elmer Sciex API 3000 triple stage quadrupole mass spectrometer equipped with a turboionspray source. Product and precursor ion analyses involved infusion of synthetic C_{12} -HFB $_{1/2}$, C_{16} -HFB $_{1/2}$, and $C_{24:1}$ -HFB $_{1/2}$ at a flow rate of 5 μ L/min. These solutions were comprised of 5 mM ammonium acetate in MeOH and 1% acetic acid. The synthetic HFB $_1$ species were present at \sim 100 fmol/ μ L. In multiple reaction monitoring (MRM) analyses, effluent from the HPLC entered the turboionspray source at a flow rate of 400 μ L/min. Dry N_2 was used as a nebulizing gas at a flow rate of 6 L/min and the face plate was heated to 500°C. In all analyses, the ion spray needle was held at 5500 V while the orifice and skimmer voltages were kept low to minimize collisional activation of molecular ions prior to entry into the first quadrupole. Product ion spectra were acquired by setting Q1 to pass the protonated molecular ion of interest. These were m/z 406.5, 588.7, 644.7, and 754.8 for HFB $_1$, C_{12} -HFB $_1$, C_{16} -HFB $_1$, and $C_{24:1}$ -HFB $_1$, respectively, as well as m/z 390.4, 572.7, 628.7, 740.8 for HFB $_2$, C_{12} -HFB $_2$, C_{16} -HFB $_2$, and $C_{24:1}$ -HFB $_2$, respectively. The $[M+H]^+$ ions were induced to dissociate by collision with N_2 in Q2 which was offset from Q1 by 35 eV. Subsequently formed product ions were detected by scanning Q3 in 0.3-u steps from m/z 50–800 with a dwell time of 1 ms. Precursor ion spectra were acquired by scanning Q1 over a 50-u window around each synthetic HFB $_{1/2}$ species estimated molecular mass in 0.1-u steps with a dwell time of 4.0 ms. Q2 was offset from Q1 by 35–65 eV to determine each species optimal collision energy with regard to formation of molecularly distinctive product ions. Therefore, Q3 was then set to pass product ions of m/z 334.4 and 336.3 for HFB $_1$ and HFB $_2$ species, respectively. Data was acquired for a total of 1 min, thus each spectrum is the signal averaged sum of 30 scans. MRM spectra were acquired by setting Q1 and Q3 to pass the precursor and product ion, respectively, which are specific to each individual species. The transitions monitored for HFB $_1$, and its *N*-acyl derivatives were m/z 406.5/334.4 (HFB $_1$), 588.7/334.4 (C_{12} -HFB $_1$), 644.7/334.4 (C_{16} -HFB $_1$), 672.7/334.4 (C_{18} -HFB $_1$), 700.7/334.4 (C_{20} -HFB $_1$), 728.7/334.4 (C_{22} -HFB $_1$), 754.8/334.4 ($C_{24:1}$ -HFB $_1$), and 756.8/334.4 (C_{24} -HFB $_1$). Q2 was offset from Q1 by 35, 45, 47.5, 47.5, 50, 52.5, 55, and 55 eV to yield optimal signal intensity for each HFB $_1$ species. The transitions monitored for HFB $_2$, C_{12} -HFB $_2$, C_{16} -HFB $_2$, and $C_{24:1}$ -HFB $_2$ were m/z 390.4/336.3, 572.7/336.6, 628.7/336.3, 738.8/336.3, respectively. Q2 was offset from Q1 by 30, 35, 40, and 50 eV to yield optimal signal for each HFB $_2$ species. The individual transitions were monitored with a dwell time of 25 ms each.

All HPLC analyses were performed using a Perkin-Elmer series 200 micropump and autosampler. Solvent A consisted of 69:30:1 v/v/v H_2O/CH_3OH /acetic acid, solvent B was

99:1 MeOH/acetic acid, and both contained 5 mM ammonium acetate. Samples were dissolved in 200 μ L solvent A, and a total of 50 μ L was injected onto a 15 cm \times 2.1 mm Supelco Discovery C18 RP column. The HFB $_{1/2}$ series were eluted at a flow rate of 400 μ L/min by pre-equilibration of the column by washing with 100% A for 2.5 min, followed by sample injection, 2-min wash with 100% A, a 5-min linear gradient to 100% B, an 8-min wash with 100% B, and a 2.5-min post-equilibration with 100% A.

The 1H NMR spectra were recorded in $CDCl_3$ on a Bruker WM 400-MHz spectrometer and are reported in parts per billions relative to $CHCl_3$ (7.26 ppm) as an internal reference.

2.3 Synthesis of *N*-lauroyl, *N*-palmitoyl- and *N*-nervonoyl-HFB $_1$

To a stirred solution of HFB $_1$ (3 mg, 7.4 μ mol), 1-hydroxybenzotriazole (HOBT; 1.1 mg, 8.2 μ mol), 1-ethyl-3-(3-dimethylaminopropyl)carbodiimide (EDC; 1.6 mg, 8.4 μ mol) and 8.2 μ mol fatty acid (1.6 mg lauric acid, 2.1 mg palmitic acid or 3.0 mg nervonic acid) in 0.5 mL DMF was slowly added *N,N*-diisopropylethylamine (2.9 mg, 22.2 μ mol). The reaction was allowed to stir overnight at room temperature under nitrogen atmosphere and product formation was checked by TLC using silica plates (Merck) and $CHCl_3$:MeOH (90:10, v/v). The fumonisins were visualized by dipping the plates into a 0.5% solution of *p*-anisaldehyde in MeOH:AcOH: H_2SO_4 (85:10:5, v/v/v) and heating them to 100°C. The reaction mixture was diluted with $CHCl_3$ to 4 mL, washed with 3 \times 2 mL of each H_2O , brine and $NaHCO_3$. The $CHCl_3$ layer was dried over Na_2SO_4 , concentrated and applied to a SiO_2 SPE cartridge (500 mg capacity; Waters) previously conditioned with 10 mL $CHCl_3$:MeOH (90:10, v/v) and 10 mL $CHCl_3$. The column was washed with 4 mL of $CHCl_3$, 4 mL of $CHCl_3$:MeOH (95:5, v/v) and eluted with 6 mL of $CHCl_3$:MeOH (90:10, v/v) in 0.5-mL steps. The fractions that contained the desired product were identified by TLC and then combined and the solvent was removed. The *N*-acylated products were characterized by ESI-MS/MS and 1H NMR.

C_{12} -HFB $_1$: yield: 3.38 mg (78%)

1H NMR (400 MHz, $CDCl_3$, ppm, *J* in Hz):

δ = 0.82 (t, *J* = 6.4, 3H), 0.87 (t, *J* = 7.0, 3H), 0.89 (t, *J* = 7.4, 3H), 0.98 (d, *J* = 7.0, 3H), 1.0–1.8 (m, 38H), 1.25 (brs, 3H), 1.94 (m, 2H), 2.34 (m, 1H), 2.56 (m, 1H), 3.3–3.9 (m, 6H)

ESI-MS: m/z 588.7 $[M+H]^+$, ESI-MS/MS (–45 eV): m/z 334.4 $[M+H-4H_2O-Acyl]^+$

C_{16} -HFB $_1$: yield: 3.30 mg (70%)

1H NMR (400 MHz, $CDCl_3$, ppm, *J* in Hz):

δ = 0.83 (d, *J* = 7.0, 3H), 0.87 (t, *J* = 6.6, 3H), 0.89 (t, *J* = 7.4, 3H), 0.99 (d, *J* = 7.0, 3H), 1.19 (d, *J* = 7.0, 3H), 1.24 (brs, 38H), 1.42 (brs, 6H), 1.8–2.0 (m, 3H), 2.18 (m, 2H),

2.34 (t, $J = 7.4$, 1H), 3.4 (dd, $J = 5.16$, 1H), 3.6–4.1 (m, 5H), 5.75 (d, $J = 8.44$, 1H)

ESI-MS: m/z 644.7 $[M+H]^+$, ESI-MS/MS (–47.5 eV): m/z 334.4 $[M+H-4H_2O-Acyl]^+$

$C_{24:1}$ -HFB₁: yield: 3.76 mg (67%)

1H NMR (400 MHz, $CDCl_3$, ppm, J in Hz):

$\delta = 0.82$ (d, $J = 6.5$, 3H), 0.87 (t, $J = 7.0$, 3H), 0.89 (t, $J = 7.0$, 3H), 0.99 (d, $J = 6.6$, 3H), 1.19 (d, $J = 6.6$, 3H), 1.25 (m, 47H), 1.4–2.4 (m, 10H), 3.39 (dd, $J = 2.9$, 8.1, 1H), 3.6–4.0 (m, 4H), 4.03 (dd, $J = 3.3$, 8.5, 1H), 5.34 (brt, $J = 4.6$, 2H)

ESI-MS: m/z 754.8 $[M+H]^+$, ESI-MS/MS (–55 eV): m/z 334.4 $[M+H-4H_2O-Acyl]^+$

2.4 Synthesis of *N*-lauroyl, *N*-palmitoyl- and *N*-nervonoyl-HFB₂

The reaction was carried out as described above with HFB₂ (2 mg, 5.1 μ mol), 1-hydroxybenzotriazole (HOBT) (0.8 mg, 5.7 μ mol), EDC (1.1 mg, 5.8 μ mol), 5.7 μ mol fatty acid (1.1 mg lauric acid, 1.5 mg palmitic acid or 2.1 mg nervonic acid), and 2.0 mg *N,N*-diisopropylethylamine (15.4 μ mol) in 0.3 mL of DMF. To eliminate any ester formation that occurred, the reaction mixture was stirred for 1 h with aqueous 1N NaOH at room temperature after extraction. For SiO_2 SPE cleanup the column was washed with 6 mL of $CHCl_3$, 2 mL of $CHCl_3$:MeOH (95:5, v/v) and eluted with 3 mL of $CHCl_3$:MeOH (95:5) and 3 mL of $CHCl_3$:MeOH (90:10) in 0.5-mL steps. The product-containing fractions were combined after identification by TLC and the solvent was removed.

C_{12} -HFB₂: yield 1.59 mg (54%)

1H NMR (400 MHz, $CDCl_3$, ppm, J in Hz):

$\delta = 0.84$ (d, $J = 7.0$, 3H), 0.87 (t, $J = 7.0$, 3H), 0.90 (t, $J = 7.4$, 3H), 0.94 (d, $J = 6.6$, 3H), 1.20 (d, $J = 7.0$, 3H), 1.0–1.8 (m, 43H), 1.25 (brs), 2.20 (t, $J = 7.7$, 1H), 3.37 (brd, $J = 5.2$, 1H), 3.45–4.05 (m, 4H)

ESI-MS: m/z 572.7 $[M+H]^+$, ESI-MS/MS (–35 eV): m/z 336.3 $[M+H-3H_2O-Acyl]^+$

C_{16} -HFB₂: yield 1.52 mg (47%)

1H NMR (400 MHz, $CDCl_3$, ppm, J in Hz):

$\delta = 0.84$ (d, $J = 7.0$, 3H), 0.87 (t, $J = 7.0$, 3H), 0.90 (t, $J = 7.4$, 3H), 0.94 (d, $J = 6.6$, 3H), 1.20 (d, $J = 7.0$, 3H), 1.0–1.4 (m, 50H), 2.21 (m, 2H), 3.36 (dd, $J = 3.5$, 8.5, 1H), 3.7–4.0 (m, 4H)

ESI-MS: m/z 628.7 $[M+H]^+$, ESI-MS/MS (–40 eV): m/z 336.3 $[M+H-3H_2O-Acyl]^+$

$C_{24:1}$ -HFB₂: yield 1.73 mg (46%)

1H NMR (400 MHz, $CDCl_3$, ppm, J in Hz):

$\delta = 0.84$ (d, $J = 6.6$, 3), 0.88 (t, $J = 7.0$, 3H), 0.90 (t, $J = 7.0$, 3H), 0.95 (d, $J = 6.3$, 3H), 1.27 (brs, 55H), 1.4–2.4 (m, 12H), 3.38 (dd, $J = 3.6$, 8.4, 1H), 3.5–3.8 (m, 3H), 4.05 (dd, $J = 3.3$, 8.4, 1H), 5.36 (brt, $J = 4.6$, 2H)

ESI-MS: m/z 738.8 $[M+H]^+$, ESI-MS/MS (–50 eV): m/z 336.3 $[M+H-3H_2O-Acyl]^+$

2.5 In vitro metabolism of HFB_{1/2} by ceramide synthase

Ceramide synthase activity was assayed following acylation of either HFB₁ or HFB₂ with palmitoyl-CoA and nervonoyl-CoA. Typically, the reaction mixture contained 25 mM potassium phosphate buffer, pH 7.4, 0.5 mM DTT, 50 μ M fatty acyl-CoA and varying concentrations of HFB₁ and HFB₂ (1 to 10 μ M, using aqueous stock solutions) in a total assay volume of 100 μ L. The enzymatic reaction was started by adding 80 μ g of microsomal protein (obtained from rat livers according to [34]) and placing the test tubes in a 37°C shaking water bath. After 15-min incubation, the reaction was stopped with 1 mL of MeOH: $CHCl_3$ (2:1) and 40 pmol of C_{12} -HFB₁ or C_{12} -HFB₂ was added as an internal standard for quantification. For product extraction, 1.25 mL of $CHCl_3$ was added, the mixture was vortexed and approximately 2 mL of slightly basic water was added. The layers were separated by centrifugation, the aqueous layer removed and the mixture washed two more times with basic water. The $CHCl_3$ layer was dried over Na_2SO_4 and evaporated to dryness using a Speed Vac. The residue was redissolved in 200 μ L of $CHCl_3$:MeOH (90:10, v/v) and 10 or 20 μ L thereof were subjected to HPLC-MS/MS analysis. For quantitative evaluation, the peak areas of the acylation products were compared with the areas of internal standards C_{12} -HFB₁/ C_{12} -HFB₂. Due to the limited amount of HFB_x, only a limited number of data points could be measured to calculate the kinetic parameters.

2.6 Inhibition of ceramide synthase

The assay was conducted as described by Merrill and Wang [35], monitoring acylation of [3H]sphingosine with palmitoyl- and nervonoyl-CoA in the presence of the *N*-acylated fumonisins. The total assay volume was 100 μ L, containing 25 mM potassium phosphate buffer, pH 7.4, 0.5 mM DTT, 50 μ M fatty acyl-CoA and either C_{16} -HFB₁, C_{16} -HFB₂, $C_{24:1}$ -HFB₁ or $C_{24:1}$ -HFB₂ (1 and 10 μ M). In a control experiment ceramide formation was assayed in the absence of *N*-acyl compounds. Background radioactivity was determined in additional controls without fatty acyl-CoA. To eliminate the risk of adhesion of sphingosine to the walls of glass reaction vessels, the assay was performed in plastic tubes. The samples were incubated for 10 min at 37°C, the enzymatic reaction stopped by adding 1 mL of MeOH: $CHCl_3$ (2:1) and the mixture base-treated with 0.1N KOH for 1 h. After addition of ceramide as carrier, lipid extraction was done as described above. After solvent evaporation, the samples were redissolved in 20 μ L of $CHCl_3$ and analyzed

by TLC. The activity of control cells was the same as has been reported earlier [18].

2.7 TLC analysis of ceramide synthase assay products

The samples were spotted onto silica plates that were developed with diethylether:MeOH (99.5:0.5, v/v). Radioactivity was detected by exposing the plates to a photographic film for 24 to 48 h at -80°C . The radioactive ceramide regions were collected and counted using a detergent-containing scintillation mixture for 10 min in a Beckman LS 7000 scintillation counter.

2.8 *In vitro* cytotoxicity

HT29 cells (ATCC, Rockville, MD) were seeded at 1×10^5 cells per 100-mm dish (Corning, Cambridge, MA), and grown in 8 mL of DMEM (Sigma) supplemented with 10% fetal calf serum (HyClone, Logan, UT), 3.5 g/L glucose, and 10 mg/L of a solution of 6.1 mg/mL penicillin G and 10 mg/mL streptomycin (Sigma) in an incubator at 37°C and a humidified atmosphere of 5% CO_2 . The medium was changed 24 h after seeding, then the cells were incubated with DMEM containing *N*-acylated aminopolyols (solubilized in 10 mL of ethanol:dodecane, 98:2; addition of this volume of ethanol:dodecane had negligible effects on cell viability). After 24 h, the cells were harvested with 0.25% trypsin in 0.05% EDTA. The number of viable cells remaining was assessed using the [3-(4,5-dimethylthiazol-2-yl)-2,5-diphenyltetrazolium bromide (MTT)] assay.

2.9 *In vivo* metabolism of HFB₁

The experimental protocol for the *in vivo* study was approved by the Animal Care and Use Committee, Richard B. Russell Agricultural Research Center, Agricultural Research Service-USDA, Athens, GA. Male Sprague-Dawley rats (Harlan, Indianapolis) were acclimated (10 days) and then randomly assigned to groups of two (controls) to three (all other groups) animals each. Rats were individually housed in stainless steel, wire-mesh cages in an environment-controlled facility (12/12 light/dark cycle) at the Richard B. Russell Agricultural Research Center, USDA. A standard rodent diet (LM-485, Teklad, Madison, WI) and tap water were provided *ad libitum*. The animals were 6 weeks of age and group mean body weights ranged from 196 (± 4.6 SD) to 198 (4.2) g at the start of the study (day 1).

Animals were given intraperitoneal injections of sterile, physiological saline (controls) or HFB₁ dissolved in sterile saline on 5 consecutive days. HFB₁ concentrations of the dosing solutions were determined by routine HPLC using OPA derivatization and fluorescence detection as described in [24]. Groups and treatments are given in the following table (Table 1).

Table 1. Experimental design of the animal study

Group	Daily dose $\mu\text{g HFB}_1$	$\mu\text{g HFB}_1/\text{kg}$ $\text{BW}^{\text{e)}$	Total dose ^{f)} $\mu\text{g HFB}_1$
Control	0 ^{a)}	0	0
Low dose	52 ^{b)}	253 ± 5	260
Mid dose	115 ^{c)}	558 ± 9	575
High dose	230 ^{d)}	1120 ± 11	1150

- a) Sterile saline, injection volume = 5 mL.
- b) HFB₁ concentration in dosing solution = 10.4 $\mu\text{g/mL}$, injection volume = 5 mL.
- c) HFB₁ concentration in dosing solution = 115 $\mu\text{g/mL}$, injection volume = 1 mL.
- d) HFB₁ concentration in dosing solution = 115 $\mu\text{g/mL}$, injection volume = 2 mL.
- e) BW, body weight; value indicates mean \pm SD; amount injected per day/average BW of the animals during the 4-day dosing period.
- f) Total amount of HFB₁ administered over 4 days.

Injection sites were rotated daily to minimize irritation. The animals were observed daily and weighed at study initiation and on day 4 (before fasting). Food consumption from study initiation through day 4 was monitored. The animals were fasted overnight prior to the last injection (day 5). Approximately 2 h after the last dose was given, both controls and two animals each from the three dosed groups were anesthetized and blood samples (approximately 2 mL, taken from the periorbital sinus) collected and stored at -80°C . The rats were then euthanized (CO_2 inhalation followed by exsanguination via the portal vein) and necropsied. The brain, gastrointestinal tract and representative samples of heart, kidney, liver and fat were collected and stored (-80°C) for analyses of *N*-acylated hydrolyzed fumonisins or quantification of sphingoid bases (liver and kidney). Additional liver and kidney samples were fixed in 10% neutral buffered formalin. After fixation, they were embedded in paraffin, sectioned (4 microns), mounted on glass slides and stained with hematoxylin and eosin for microscopic examination. The remaining low-dose, mid-dose and high-dose rats were observed and weighed weekly for an additional 3 weeks. At the end of this “wash out” period, they were killed and tissue samples collected as described above.

2.10 Extraction of tissues

Samples (100 mg of tissue) were homogenized in 0.9 mL of PBS and 0.2-mL aliquots were transferred to four glass test tubes (16 \times 100 mm). To extract the lipids 2.4 mL of CHCl_3 :MeOH (1:2) and standards (0.5 nmol of each of C₂₀-sphingosine, C₁₂-ceramide and C₁₂-HFB₁) was added. The mixture was vortexed, 2.4 mL of CHCl_3 and 5 mL of H_2O were added to split into two phases, the mixture was vortexed again and centrifuged. The CHCl_3 layer was removed and the aqueous phase was re-extracted three times, each with 1 mL of CHCl_3 . The combined CHCl_3 extracts were

dried, evaporated to dryness using a Speed Vac, dissolved in 0.1 mL of 0.1 M KOH in methanol, and incubated for 2 h at 37°C. One microliter of CHCl₃ was added, the mixture was centrifuged to remove insoluble material, then transferred to a new glass test tube, dried using a Speed Vac and dissolved in 200 µL of solvent A for HPLC-MS/MS analysis.

2.11 Statistics

All analyses were conducted at least in triplicate and the results are given as mean values ± SE. The statistical significance of differences was determined by the unpaired Student's *t*-test using SigmaPlot. The kinetic parameters were derived from linear regression analyses of the data.

3 Results

As HFB₁ is known to be acylated by ceramide synthase using palmitoyl-CoA, the initial experiments investigated the acylation of HFB₁ and HFB₂ to determine if both types of fumonisins were handled this way as well as compared palmitoyl (C₁₆)-CoA and nervonoyl (C_{24:1})-CoA as the fatty acyl-CoA cosubstrate. Nervonoyl-CoA was chosen due to its relative abundance within the very-long-chain ceramide fraction of sphingolipids [35, 36] as well as because its utilization would indicate that more than one CerS isoform is able to acylate these compounds [29].

3.1 Analysis of acylation products by HPLC-MS/MS

A new method based on HPLC-ESI-MS/MS was developed for the detection and qualitative and quantitative analysis of the HFB_{1/2} acylation products. The possibly formed products *N*-palmitoyl- and *N*-nervonoyl-HFB₁ (C₁₆/C_{24:1}-HFB₁) and -HFB₂ (C₁₆/C_{24:1}-HFB₂) as well as *N*-lauroyl-HFB₁ and -HFB₂ (C₁₂-HFB_{1/2}), for use as internal standards, were synthesized (structures see Fig. 1), their fragmentation in the MS/MS spectrometer were studied and the characteristic product ions were used for the setup of suitable MRM experiments. The electrospray mass spectra of all compounds showed the protonated molecular ions [M+H]⁺ at *m/z* 588.7, 644.7 and 754.8 for C₁₂-HFB₁, C₁₆-HFB₁ and C_{24:1}-HFB₁ and at *m/z* 572.7, 628.7 and 738.8 for C₁₂-HFB₂, C₁₆-HFB₂ and C_{24:1}-HFB₂. Fragmentation of the protonated molecular ions resulted in the cleavage of the fatty acyl chain and successive loss of several water molecules, thus yielding an [M+H-4H₂O-acyl]⁺ ion at *m/z* 334.4 as the predominant product ion for the HFB₁ series. Figure 2 shows a product ion spectrum of C_{24:1}-HFB₁ with the typical fragmentation yielding the characteristic ion at *m/z* 334.4. The HFB₂ compounds showed an [M+H-3H₂O-acyl]⁺ at *m/z* 336.3 as the major fragmentation product. These characteristic product ions were employed for MRM experiments.

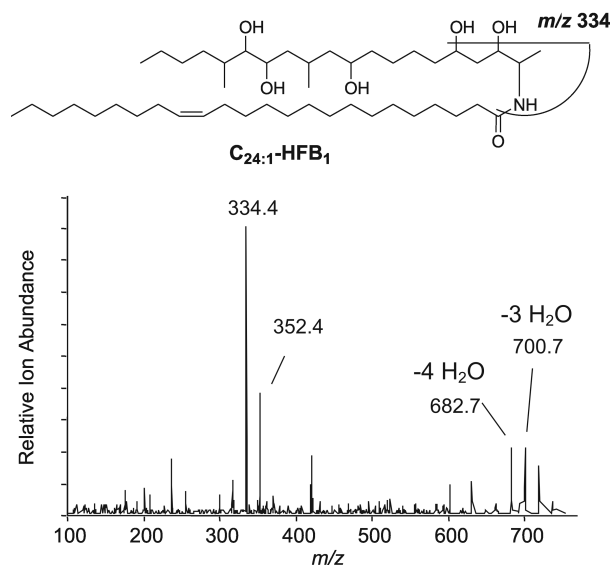


Figure 2. Product ion spectrum and fragmentation of *N*-nervonoyl-HFB₁ (C_{24:1}-HFB₁) (collision gas N₂, offset voltage 35 eV).

The analysis of sample material required the separation of the acylation products from interfering matrix components. For this purpose, chromatographic methods had to be developed for both the HFB₁ and HFB₂ series. Quantitative evaluation was carried out by comparison of the peak areas with those of the internal standards C₁₂-HFB₁ and C₁₂-HFB₂ after validation that under the optimized MRM conditions each gave similar ion yields. With an LOD of about 10 fmol/µL the sensitivity of the developed method was well sufficient for a reliable analysis.

3.2 Acylation of HFB₁ and HFB₂ by ceramide synthase(s)

Incubation of rat liver microsomes with HFB₁ or HFB₂ and either nervonoyl- or palmitoyl-CoA resulted in the formation of the respective acylation product, namely *N*-nervonoyl-HFB₁ (C_{24:1}-HFB₁) and -HFB₂ (C_{24:1}-HFB₂) and *N*-palmitoyl-HFB₁ (C₁₆-HFB₁) and -HFB₂ (C₁₆-HFB₂), all of which were unambiguously identified in the MRM experiments via their protonated molecular ions and characteristic product ions. Most remarkably, a comparison of the occurring product amounts showed that acylation of HFB₁ as well as HFB₂ is faster with nervonoyl-CoA than with the palmitoyl coenzyme. Figure 3 illustrates the amounts of acylation products obtained at two different substrate concentrations. In the case of HFB₁, five- and tenfold more C_{24:1}-HFB₁ than C₁₆-HFB₁ was formed at 2 and 10 µM HFB₁, respectively. Similarly, the formation of C_{24:1}-HFB₂ exceeded that of C₁₆-HFB₂ by factors of 3 (2 µM) and 7 (10 µM). HFB₁ and HFB₂ were equally well accepted as substrates by ceramide synthase, hence, the results are expressed for “HFB_{1/2}” where the findings apply to both.

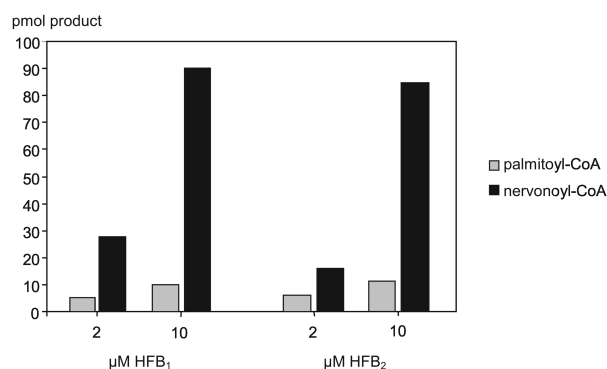


Figure 3. Amounts of acylation products obtained by incubation of rat liver microsomes with nervonoyl- and palmitoyl-CoA and HFB₁ or HFB₂ at two different concentrations.

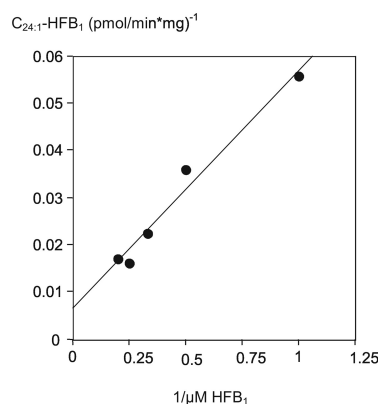


Figure 4. Double reciprocal plot of acylation of HFB₁ by rat liver microsomes using varying concentrations of HFB₁ and 50 μM nervonoyl-CoA.

The formation of C_{24:1}-HFB₁ and C₁₆-HFB₁ followed a simple Michaelis-Menten relationship. A double reciprocal (Lineweaver-Burk) plot was chosen for linearization in order to determine the characteristic kinetic parameters. For C_{24:1}-HFB₁ formation, the apparent K_m was 7.9 μM and v_{max} was 157 pmol/min/mg microsomal protein (Fig. 4), whereas the acylation of HFB₁ with palmitoyl-CoA occurred with a K_m of 1.2 μM and at a v_{max} of 8.7 pmol/min/mg protein (Fig. 5). Expressed as v_{max}/K_m, the formation of C_{24:1}-HFB₁ (19.9) was approximately twofold higher than formation of C₁₆HFB₁ (7.3). Unfortunately, it was not possible to determine K_m and v_{max} for the acylation of HFB₂ due to the limited availability of substrate.

3.3 Cytotoxicity of *N*-acylated hydrolyzed fumonisins to HT29 cells

The cytotoxicity of the ceramide synthase acylation products C₁₆-HFB₁, C_{24:1}-HFB₁, C₁₆-HFB₂ and C_{24:1}-HFB₂ was determined by incubation of each compound with HT29 cells, a human colonic cell line sensitive to FB₁ and HFB₁ [23]. Figure 6 summarizes the results. All substances sig-

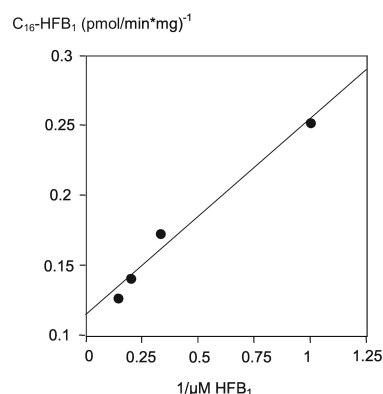


Figure 5. Double reciprocal plot of acylation of HFB₁ by rat liver microsomes using varying concentrations of HFB₁ and 50 μM palmitoyl-CoA.

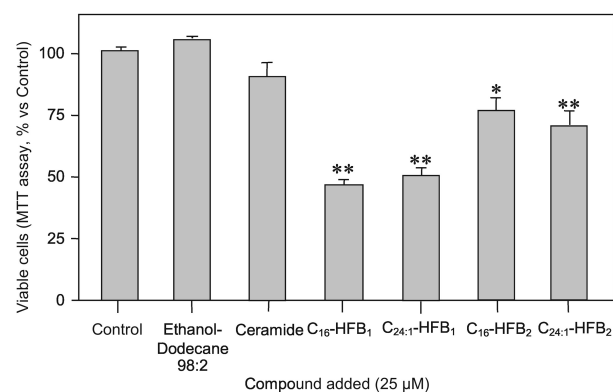


Figure 6. Toxicity of *N*-acylated aminopolyols on HT29 cells at a concentration of 25 μM (**p* < 0.05; ***P* < 0.01; vs. ethanol-dodecane 98:2). The results are shown as mean ± SE (*n* = 3) (Control: cell medium, ethanol-dodecane: control containing the solvent carrier, ceramide: control with 25 μM C2-ceramide).

nificantly reduced the number of viable cells at a concentration of 25 μM. After 24-h incubation, C₁₆-HFB₁ and C_{24:1}-HFB₁ caused a 50% reduction in the number of viable cells and were therefore more potent than C₁₆-HFB₂ and C_{24:1}-HFB₂, which caused a 30% reduction. Although the MTT assay cannot distinguish between reduced cell viability due to cytotoxicity and lower cell numbers due to growth inhibition, the results clearly demonstrate that the *N*-acylated metabolites are more potent compared to FB₁ and HFB₁ [23, 28].

3.4 Inhibition of ceramide synthase by *N*-acylated hydrolyzed fumonisins

Because inhibition of ceramide synthase(s) appears to be a key step in the toxicity of fumonisins, we also evaluated the acylation products' ability to inhibit ceramide formation. Thus, the ceramide synthase-mediated acylation of [³H]sphingosine with palmitoyl- or nervonoyl-CoA was

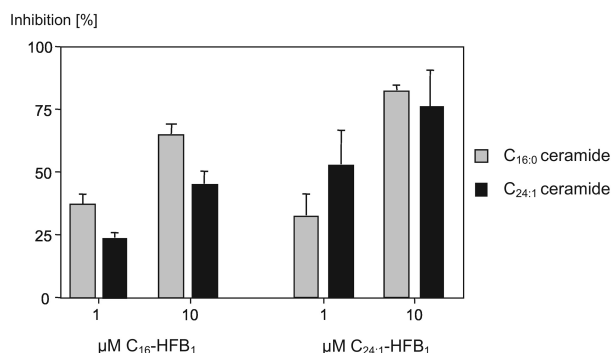


Figure 7. Inhibition of ceramide synthase activity, measured using the acylation of [³H]sphingosine, by C₁₆-HFB₁ and C_{24:1}-HFB₁ at 1 and 10 μM. The data are shown as the mean ± SE (*n* = 3–5).

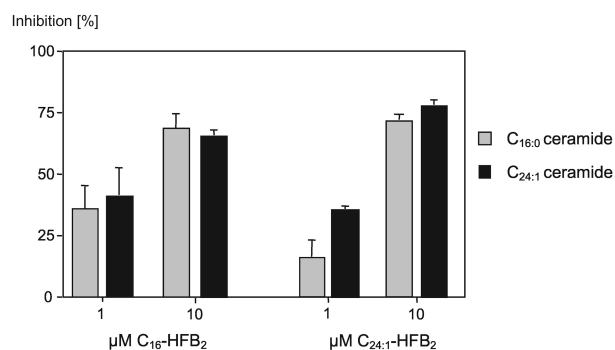


Figure 8. Inhibition of ceramide synthase activity, measured using the acylation of [³H]sphingosine, by C₁₆-HFB₂ and C_{24:1}-HFB₂ at 1 and 10 μM. The data are shown as the mean ± SE (*n* = 3–5).

monitored in the presence of 1 and 10 μM C_{24:1}-HFB₁, C_{24:1}-HFB₂, C₁₆-HFB₁ or C₁₆-HFB₂. At concentrations of 1 μM, the HFB₁ compounds inhibited ceramide synthase activity by 30% (Fig. 7) while up to 80% inhibition was observed at 10 μM. C₁₆-HFB₂ and C_{24:1}-HFB₂ acted similarly, causing 30 and 70% inhibitions at 1 and 10 μM, respectively (Fig. 8). These findings are in agreement with the results of the cytotoxicity tests, suggesting that the acylated hydrolyzed fumonisins might exert toxic effects via a similar mode of action as FB₁.

3.5 *In vivo* acylation of HFB₁ and HFB₂

Because HFB₁ and HFB₂ are acylated *in vitro* by the ceramide synthase(s) to form *N*-acyl-metabolites with cytotoxic and ceramide synthase inhibitory potential, the formation of these metabolites was investigated *in vivo*. Blood and tissues from rats that had been administered HFB₁ (at 52, 115 and 230 μg/day, intraperitoneal) for 5 days were extracted as described in Section 2.10 and analyzed by HPLC-MS/MS. Interestingly, several *N*-acyl-metabolites were found. Figure 9 shows an HPLC-MRM-MS chromatogram of a rat

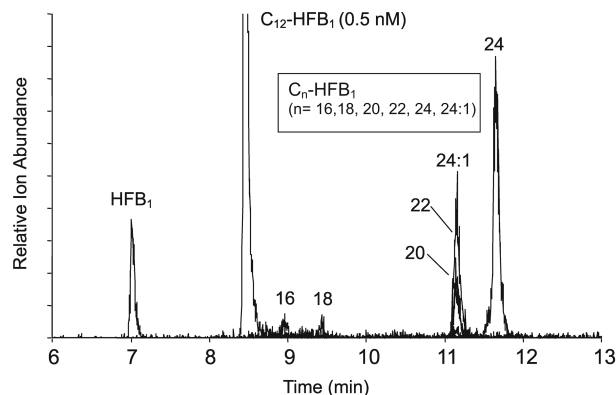


Figure 9. HPLC-MRM-MS chromatogram of a rat liver extract from an animal of the high-dose group (230 μg HFB₁/day). Several *N*-acyl-HFB₁-metabolites (C_{*n*}-HFB₁) with fatty acids of various chain length could be detected (C₁₂-HFB₁: internal standard) (structures see Fig. 1).

liver extract from an animal of the high dose group (230 μg HFB₁/day). Besides residual HFB₁ and the C₁₂-HFB₁ internal standard, HFB₁ acylation products with fatty acids of various chain lengths were unambiguously identified. The most prevalent species found were the HFB₁-acyl compounds containing long-chain fatty acids (C₂₄, C_{24:1}, C₂₂ and C₂₀). Lesser amounts of the respective metabolites with C₁₆ and C₁₈ fatty acids were also detected (structures see Fig. 1).

Acylation products were not found in the control animals, indicating that their formation occurred as a result of the exposure to HFB₁. In addition, no *N*-acyl-metabolites were found in the animals analyzed three weeks after the last dose was given, indicating that the acylated-HFB_{1/2} metabolites were further metabolized and/or excreted. The quantitative evaluation of the data from the individual rats of the three dose groups is summarized in Fig. 10. The liver and kidney (data not shown) of all animals had a similar distribution pattern for the fatty acids found in the metabolites, with the C₂₄-compound occurring in the highest amounts (up to 2.4 nmol/g), followed by C_{24:1}-HFB₁ (up to 0.8 nmol/g) and C₂₂ (0.25 nmol/g). C₁₆-HFB₁ and C₁₈-HFB₁ were detected in only a few of the animals, and in those cases typically at the order of 0.04 to 0.13 nmol/g (with the highest amounts being 0.17 and 0.54 nmol/g, respectively). The low amounts of the latter metabolites were not correlated with the dose and therefore were probably due to variations in ceramide synthase subtypes among individual animals.

Gross and microscopic examinations of the liver and kidney, which are the major target organs of fumonisins in rats, from the animals killed on day 5 did not reveal any treatment-related alterations. Body weight, food consumption, and kidney and liver weights of all groups were likewise similar (data not shown). Thus, the intraperitoneal (ip) doses used in this short-term experiment, which ranged up to 1.12 mg/kg body weight, were insufficient to cause overt tissue damage. The bioavailability of HFB₁ is not known

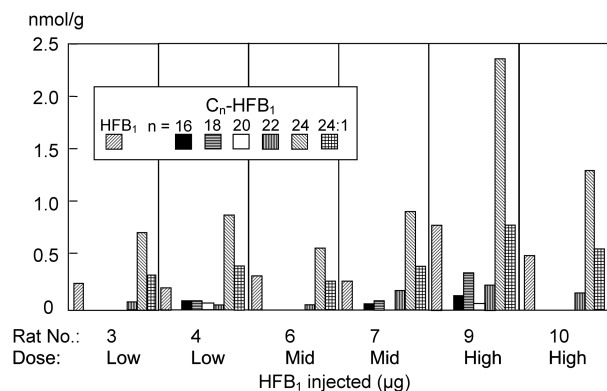


Figure 10. Distribution of *N*-acyl-HFB₁-metabolites (C_n-HFB₁) of various fatty acid chain lengths in the livers of six rats that had been given low [52 μg/kg body weight (BW)], mid (115 μg/kg BW) or high (230 μg/kg BW) intraperitoneal (ip) doses of HFB₁ for 4 consecutive days. No *N*-acyl-HFB₁-metabolites were found in the livers of control animals (rats No. 1 and 2) or in rats 5 (low dose), 8 (mid dose) and 11 (high dose), which were killed 3 weeks after the last day of dosing (structures see Fig. 1).

but is considerably higher than that of FB₁ [37]. Therefore, the dietary HFB₁ concentrations corresponding to our ip doses cannot be calculated but could have ranged from 10 ppm (if gastrointestinal absorption approaches 100%) to about 200 ppm (bioavailability of 5%) at the high-dose level (Group B2). An intermediate value is likely [37].

4 Discussion

Recently, we identified *N*-palmitoyl-HFB₁ (C₁₆-HFB₁) as the cytotoxic product from the acylation of HFB₁ with palmitoyl-CoA by ceramide synthase *in vitro* [28]. We have now identified *N*-nervonoyl-HFB₁ (C_{24:1}-HFB₁), *N*-palmitoyl- and *N*-nervonoyl-HFB₂ (C₁₆-HFB₂, C_{24:1}-HFB₂) as new metabolites formed by ceramide synthase with hydrolyzed fumonisins HFB₁ and HFB₂ *in vitro*. Acylation apparently does not detoxify hydrolyzed fumonisins because C₁₆-HFB₁, C₁₆-HFB₂, C_{24:1}-HFB₁ and C_{24:1}-HFB₂ metabolites were cytotoxic for HT29 cells as well as inhibited ceramide synthase *in vitro*.

These results demonstrate that HFB₁ and HFB₂ are acylated *in vitro* and *in vivo*. It is likely that the enzyme(s) that are responsible for acylation are ceramide synthases because HFB_{1/2} are inhibitors of sphingosine acylation as well as themselves acylated, as expected for substrate competitive inhibitors. If so, it remains intriguing that even though these compounds differ from the natural substrates sphinganine and sphingosine in the stereochemistry at C2 and C3 (the carbon atoms in the vicinity of the group to be modified) and other structural elements (the absence of the hydroxyl group at C1 and the presence of an hydroxyl function at C5), the enzyme(s) are still able to use HFB₁ and HFB₂ as substrates.

This agrees with results of studies using various stereoisomers of sphinganine and synthetic 1-deoxy-5-hydroxy-sphinganine as substrates for ceramide synthase that have concluded that both *erythro* and *threo* isomers are reasonably well accommodated by these enzymes [28, 38].

A comparison of the apparent v_{\max} showed that acylation with nervonoyl-CoA is 18-fold faster than with palmitoyl-CoA, or >2-fold better utilized when v_{\max}/K_m are compared. Importantly, HPLC-MS/MS analysis of the liver samples from rats dosed with HFB₁ has demonstrated for the first time that *N*-acyl-HFB₁-metabolites (C_n-HFB₁) with fatty acids of various chain lengths (C₁₆, C₁₈, C₂₀, C₂₂, C₂₄ and C_{24:1}) are also formed *in vivo*. The preferred acylation by C_{24:1}-fatty acyl-CoA *in vitro* and the finding that mainly very-long-chain *N*-acyl-HFB₁-metabolites are formed *in vivo* (Figs. 9 and 10) may be interpreted in the context of recent findings that mammals have multiple ceramide synthase genes (*Lass* 1–6 recently named CerS1–6), showing a different specificity concerning the fatty acyl-CoA (for a review see [29]). It was first shown that overexpression of LASS1 (CerS1) resulted in a selective increase in C18-ceramide in mammalian cells [30]. Subsequently, LASS4 (CerS4) and LASS5 (CerS5) were shown to selectively utilize C_{18/20} and C₁₆ acyl-CoAs, respectively [31, 32], LASS6 to produce shorter chain ceramides (C₁₄ and C₁₆) [39] and LASS3 to produce very-long-chain ceramides (C₁₈, C₂₄) (and LASS2, CerS2, appears to be relatively nonspecific) [40]. It is not known why mammals have multiple CerS genes, but it implies an important role for ceramides containing specific fatty acids. The preferred formation of very-long-chain *N*-acyl-HFB₁-metabolites – as shown in the liver (Figs. 9 and 10) – implies that CerS2 and CerS3, which appear to be most active with the corresponding fatty acyl-CoA, may be the enzyme(s) that are most involved in acylation of the hydrolyzed fumonisins, either because these can best accommodate the HFB_{1/2} molecules or perhaps due to these being the major LASS (CerS) genes that are expressed in the tissues. Future studies could use genetic approaches, such as suppression of individual LASS (CerS) proteins using siRNA, to test this hypothesis. Studies on the toxic effects of hydrolyzed fumonisins have yielded mixed results. Liver and kidney lesions and liver tumor promoting activity have been demonstrated in rats fed hydrolyzed *Fusarium* culture materials containing hydrolyzed fumonisins, but no detectable (HPLC) FB₁ or FB₂ [24, 25]. In these studies, the potency of HFB₁ was about equal to or less than that of FB₁. In contrast, Collins *et al.* [27] reported that HFB₁ did not induce tissue lesions or affect sphingoid bases when given orally to pregnant rats. Howard *et al.* [26] also found no evidence that HFB₁ was toxic when fed at concentrations of ca. 29 and 58 ppm (corresponding to 70 and 140 μmol/kg diet, respectively) to female mice for 28 days. In contrast, FB₁ caused hepatic lesions and affected sphingolipid metabolism at these (μmol/kg diet) concentrations. The reason that the findings of Hendrich *et al.* [25] and Voss *et al.* [24] do not

agree with those of Collins *et al.* [27] and Howard *et al.* [26] is not known. One possibility is that matrix-bound or “hidden” FB₁, which could become bioavailable during digestion, may have been present in the culture materials (reviewed in [41]). Differences in dosing protocols and/or physiological differences among the species and, within species, the strains of animals used in the experiments are also possible. The latter could include differences in ability of the animals to acylate the hydrolyzed fumonisins. Therefore, studies comparing the metabolism of HFB₁ in rats and mice would be of interest because they might reveal that the reported differences in sensitivity of mice and rats to HFB₁ might depend on the extent and type of metabolism.

There is evidence indicating that fumonisins are potential risk factors for cancer or neural tube (birth) defects in humans but an unequivocal relationship between human disease and exposure to fumonisins or hydrolyzed fumonisins has not been established. However, that HFB₁ and the acylation products are reducing the number of viable HT29 cells, suggests that consumption of fumonisins or hydrolyzed fumonisins might adversely affect the human gastrointestinal tract or other tissues. Following oral administration (gavage) of FB₁ to non-human primates, a portion of the dose recovered in the intestinal epithelial cells, excreta, bile and gut contents consisted of HFB₁ and partially hydrolyzed FB₁ [42] and, based on our cytotoxicity results, hydrolyzed fumonisins or their metabolites might damage the gut epithelium. Furthermore, according to one report [37], the bioavailability of HFB₁ in rats is greater than that of FB₁, increasing the likelihood that HFB₁, either injected via contaminated alkali-processed corn products [41] or formed by hydrolysis of FB₁ in the gastrointestinal tract can be absorbed by the gut and thereby allow subsequent metabolism to C_{24:1}-HFB₁ and C₁₆-HFB₁ in the liver or other tissues to enhance its biological effects.

In summary, we have demonstrated that HFB₁ and HFB₂ are metabolized by microsomes *in vitro* and (at least) HFB₁ by rats *in vivo* to acylated derivatives that resemble ceramide in structure. These compounds reduce the number of viable HT29 cells and inhibit ceramide synthase and, as a result, warrant further investigations on the role they might play in the toxicity of hydrolyzed fumonisins.

This study was supported by the Deutsche Forschungsgemeinschaft, Bonn (HU 730/1-6)(H.-U.H.) and GM076217 (A.H.M.)

5 References

- [1] Marasas, W. F. O., Discovery and occurrence of the fumonisins: A historical perspective, *Environ. Health Perspect.* 2001, 109 (Suppl. 2), 239–243.
- [2] Rheeder, J. P., Marasas, W. F. O., Vismer, H. F., Production of fumonisin analogs by *Fusarium* species, *Appl. Environ. Microbiol.* 2002, 68, 2101–2105.
- [3] Hopmans, E. C., Murphy, P. A., Detection of fumonisins B₁, B₂, and B₃ and hydrolyzed fumonisin B₁ in corn-containing foods, *J. Agric. Food Chem.* 1993, 41, 1655–1658.
- [4] Hartl, M., Humpf, H.-U., Simultaneous determination of fumonisin B₁ and hydrolyzed fumonisin B₁ in corn products by liquid chromatography/electrospray ionization mass spectrometry, *J. Agric. Food Chem.* 1999, 47, 5078–5083.
- [5] Marasas, W. F. O., Kellerman, T. S., Gelderblom, W. C. A., Coetzer, J. A. W., *et al.*, Leukoencephalomalacia in a horse induced by fumonisin B₁ isolated from *Fusarium moniliforme*, *Onderstepoort J. Vet. Res.* 1988, 55, 197–203.
- [6] Kellerman, T. S., Marasas, W. F. O., Thiel, P. G., Gelderblom, W. C. A., *et al.*, Leukoencephalomalacia in two horses induced by oral dosing of fumonisin B₁, *Onderstepoort J. Vet. Res.* 1990, 57, 269–275.
- [7] Harrison, L. R., Colvin, B. M., Greene, J. T., Newman, L. E., *et al.*, Pulmonary edema and hydrothorax in swine produced by fumonisin B₁, a toxic metabolite of *Fusarium moniliforme*, *J. Vet. Diagn. Invest.* 1990, 2, 217–221.
- [8] Haschek, W. M., Gumprecht, L. A., Smith, G., Tumbleson, M. E., *et al.*, Fumonisin toxicosis in swine: An overview of porcine pulmonary edema and current perspectives, *Environ. Health Perspect.* 2001, 109 (Suppl. 2), 251–257.
- [9] Voss, K. A., Riley, R. T., Norred, W. P., Bacon, C. W., *et al.*, An overview of rodent toxicities: Liver and kidney effects of fumonisins and *Fusarium moniliforme*, *Environ. Health Perspect.* 2001, 109 (Suppl. 2), 259–266.
- [10] Gelderblom, W. C. A., Kriek, N. P. J., Marasas, W. F. O., Thiel, P. G., Toxicity and carcinogenicity of the *Fusarium moniliforme* metabolite, fumonisin B₁ in rats, *Carcinogenesis* 1991, 12, 1247–1251.
- [11] Gelderblom, W. C. A., Abel, S., Smuts, C. M., Marnewick, J., *et al.*, Fumonisin-induced hepatocarcinogenesis: Mechanisms related to cancer initiation and promotion, *Environ. Health Perspect.* 2001, 109 (Suppl. 2), 291–300.
- [12] Howard, P. C., Eppley, R. M., Stack, M. E., Warbritton, A., *et al.*, Fumonisin B₁ carcinogenicity in a two-year feeding study using F344 rats and B6C3F(1) mice, *Environ. Health Perspect.* 2001, 109 (Suppl. 2), 277–282.
- [13] NTP study, NIH Publication No. 99-3955, US Department of Health and Human Services, National Institutes of Health, 1999.
- [14] Chu, F. S., Li, G. Y., Simultaneous occurrence of fumonisin B₁ and other mycotoxins in moldy corn collected from the People's Republic of China in regions with high incidences of esophageal cancer, *Appl. Environ. Microbiol.* 1994, 60, 847–852.
- [15] Rheeder, J. P., Marasas, W. F. O., Thiel, P. G., Sydenham, E. W., *et al.*, *Fusarium moniliforme* and fumonisins in corn in relation to human esophageal cancer in Transkei, *Phytopathology* 1992, 82, 353–357.
- [16] Marasas, W. F. O., Riley, R. T., Hendricks, K. A., Stevens, V. L., *et al.*, Fumonisin disrupt sphingolipid metabolism, folate transport, and neural tube development in embryo culture and *in vivo*, a potential risk factor for human neural tube defects among populations consuming fumonisin-contaminated maize, *J. Nutr.* 2004, 134, 711–716.
- [17] Missmer, S. A., Suarez, L., Felkner, M., Wang, E., *et al.*, Exposure to fumonisins and the occurrence of neural tube defects along the Texas-Mexico border, *Environ. Health Perspect.* 2006, 114, 237–241.

- [18] Wang, E., Norred, W. P., Bacon, C. W., Riley, R. T., *et al.*, Inhibition of sphingolipid biosynthesis by fumonisins. Implications for diseases associated with *Fusarium moniliforme*, *J. Biol. Chem.* 1991, 266, 14486–14490.
- [19] Merrill, A. H., Jr., Sullards, M. C., Wang, E., Voss, K. A., *et al.*, Sphingolipid metabolism: Roles in signal transduction and disruption by fumonisins, *Environ. Health Perspect.* 2001, 109 (Suppl. 2), 283–289.
- [20] Riley, R. T., Enongene, E., Voss, K. A., Norred, W. P., *et al.*, Sphingolipid perturbations as mechanisms for fumonisin carcinogenesis, *Environ. Health Perspect.* 2001, 109 (Suppl. 2), 301–308.
- [21] Desai, K., Sullards, M. C., Allegood, J., Wang, E., *et al.*, Fumonisin and fumonisin analogs as inhibitors of ceramide synthase and inducers of apoptosis *Biochim. Biophys. Acta* 2002, 1585, 188–192.
- [22] Riley, R., Voss, K. A., Differential sensitivity of rat kidney and liver to fumonisin toxicity: organ-specific differences in toxin accumulation and sphingoid base metabolism, *Toxicol. Sci.* 2006, 92, 335–345.
- [23] Schmelz, E. M., Dombrink-Kurtzman, M. A., Roberts, P. C., Kozutsumi, Y., *et al.*, Induction of apoptosis by fumonisin B₁ in HT29 cells is mediated by the accumulation of endogenous free sphingoid bases, *Tox. Appl. Pharm.* 1998, 148, 252–260.
- [24] Voss, K. A., Bacon, C. W., Meredith, F. I., Norred, W. P., Comparative subchronic toxicity studies of nixtamalized and water extracted *Fusarium moniliforme* culture material, *Food Chem. Toxicol.* 1996, 34, 623–632.
- [25] Hendrich, S., Miller, K. A., Wilson, T. M., Murphy, P. A., Toxicity of *Fusarium proliferatum*-fermented nixtamalized corn-based diets fed to rats: Effect of nutritional status, *J. Agric. Food Chem.* 1993, 41, 1649–1654.
- [26] Howard, P. C., Couch, L. H., Patton, R. E., Eppley, R. M., *et al.*, Comparison of the toxicity of several fumonisin derivatives in a 28-day feeding study with female B6C3F(1) mice, *Toxicol. Appl. Pharmacol.* 2002, 185, 153–165.
- [27] Collins, T. F., Sprando, R. L., Black, T. N., Olejnik, N., *et al.*, Effects of aminopentol on in utero development in rats, *Food Chem Toxicol.* 2006, 44, 161–169.
- [28] Humpf, H.-U., Schmelz, E. M., Meredith, F. I., Vesper, H. *et al.*, Acylation of naturally occurring and synthetic 1-deoxy-sphinganine by ceramide synthase – Formation of *N*-palmitoyl-aminopentol produces a toxic metabolite of hydrolyzed fumonisin, AP₁, and a new category of ceramide synthase inhibitor, *J. Biol. Chem.* 1998, 273, 19060–19064.
- [29] Pewzner-Jung, Y., Ben-Dor, S., Futerman, A. H., When do Lasses (longevity assurance genes) become CerS (ceramide synthases)? Insights into the regulation of ceramide synthesis, *J. Biol. Chem.* 2006, 281, 25001–25005.
- [30] Venkataraman, K., Riebeling, C., Bodennec, J., Riezman, H., *et al.*, Upstream of growth and differentiation factor 1 (uog1), a mammalian homolog of the yeast longevity assurance gene 1 (LAG1), regulates *N*-stearoyl-sphinganine (C18-(dihydro)-ceramide) synthesis in a fumonisin B₁-independent manner in mammalian cells, *J. Biol. Chem.* 2002, 277, 35642–35649.
- [31] Riebeling, C., Allegood, J. C., Wang, E., Merrill, A. H., Jr., Futerman, A. H., Two mammalian longevity assurance gene (LAG1) family members, trh1 and trh4, regulate dihydroceramide synthesis using different fatty acyl-CoA donors, *J. Biol. Chem.* 2003, 278, 43452–43459.
- [32] Lahiri, S., Futerman, A. H., LASS5 is a bona fide dihydroceramide synthase that selectively utilizes palmitoyl-CoA as acyl donor, *J. Biol. Chem.* 2005, 280, 33735–33738.
- [33] Hopmans, E. C., Hauck, C. C., Hendrich, S., Murphy, P. A., Excretion of fumonisin B₁, hydrolyzed fumonisin B₁, and the fumonisin B₁-fructose adduct in rats, *J. Agric. Food Chem.* 1997, 45, 2618–2625.
- [34] Merrill, A. H., Jr., Wang, E., Enzymes of ceramide biosynthesis, *Methods Enzymol.* 1992, 209, 427–437.
- [35] Wang, E., Merrill, A. H., Jr., Ceramide synthase, *Methods Enzymol.* 1999, 311, 15–21.
- [36] Merrill, A. H., Jr., Sweeley, C. C., Sphingolipids: Metabolism and cell signalling. In: Vance, D. E., Vance, J. E. (Eds.), *New Comprehensive Biochemistry: Biochemistry of lipids, lipoproteins, and membranes*. Elsevier Science, Amsterdam 1996, 31, 309–338.
- [37] Dantzer, W. R., Hopper, J., Mullin, K., Hendrich, S., Murphy, P. A., Excretion of ¹⁴C-fumonisin B₁, ¹⁴C-hydrolyzed fumonisin B₁, and ¹⁴C-fumonisin B₁-fructose in rats, *J. Agric. Food Chem.* 1999, 47, 4291–4296.
- [38] Stoffel, W., Bister, K., Stereospecificities in the metabolic reactions of the four isomeric sphinganine (dihydrosphingosines) in rat liver, *Hoppe-Seyler's Z. Physiol. Chem.* 1973, 354, 169–181.
- [39] Mizutani, Y., Kihara, A., Igarashi, Y., Mammalian Lass6 and its related family members regulate synthesis of specific ceramides, *Biochem. J.* 2005, 390, 263–271.
- [40] Mizutani, Y., Kihara, A., Igarashi, Y., LASS3 (longevity assurance homologue 3) is a mainly testis-specific (dihydro)-ceramide synthase with relatively broad substrate specificity, *Biochem. J.* 2006, 398, 531–538.
- [41] Humpf, H.-U., Voss, K. A., Effects of thermal food processing on the chemical structure and toxicity of fumonisin mycotoxins, *Mol. Nutr. Food Res.* 2004, 48, 255–269.
- [42] Shephard, G. S., Thiel, P. G., Sydenham, E. W., Alberts, J. F., Cawood, M. E., Distribution and excretion of a single dose of the mycotoxin fumonisin B₁ in a nonhuman primate, *Toxicol.* 1994, 32, 735–741.